Working Paper No. 42/04

Understanding the Stochastics of Nodal Prices: Price Processes in a Constrained Network

by

Arne-Christian Lund
Linda Rud

SNF-Project No. 7165
Long-run Environmental and Economic Efficiency in Competitive Power Markets:
Optimal Investments in Distributed Generation, Renewables and Network Capacity.

The project is financed by Research Council of Norway

INSTITUTE FOR RESEARCH IN ECONOMICS AND BUSINESS AMINISTRATION
NOVEMBER 2004
ISSN 1503-2140

Understanding the Stochastics of Nodal Prices: Price Processes in a Constrained Network

Arne-Christian Lund and Linda Rud*

Abstract

Network congestion in competitive electricity markets may be managed by geographically differentiated nodal prices. The stochastics of an unconstrained equilibrium price reflect the underlying fundamentals of demand and supply. The stochastics of nodal prices in addition reflect the consequences of grid congestion. This paper demonstrates how a static three-node model may be combined with dynamic modelling of fundamental parameters, giving stochastic nodal price processes consistent with the underlying grid. These price processes may be employed in analysing production, hedging, and investment decisions under uncertainty.

1 Introduction

Electricity prices in competitive markets have proven to be highly volatile. A thorough understanding of the stochastic price processes is important in e.g. production planning, risk management and investment planning. The stochastics of equilibrium commodity prices in general reflect the stochastic nature of the underlying fundamentals of demand and supply. For electricity, however, a special factor is the effect of the constraints in the underlying grid. By simply clearing the market on a common equilibrium price, often denoted the *system price*, the resulting allocation of production and consumption may be infeasible due to grid congestion. In the case of congestion a feasible market solution may be obtained by clearing the market on differentiated nodal prices[1]. Optimal nodal prices may be characterized as the

*The authors would like to thank Mette Bjørndal for important contributions.

[1] The concept of nodal electricity prices is first discussed in Schweppe et al. [7].

prices that optimize the aggregate social surplus implied by the bid curves, *within* the capacity constraints of the grid. For the individual consumers and producers, the relevant prices processes are the area/nodal specific prices, not the system price process. The objective of our paper is to gain insight into the impact of grid limitations on the stochastic nodal price processes.

In literature, there have been two main approaches to modelling electricity prices. Firstly, there are several contributions which focus on finding appropriate stochastic processes to model a given time series of electricity prices. The processes are in turn applied to e.g. valuing contingent claims. For example, Lucia and Schwartz [4] study the use of different one and two factor models in modelling the system spot price on NordPool spot exchange. These processes are fitted to data, and then used to value futures and forward contracts. Weron et al. [8] formulates a jump diffusion model, and a regime switching model for the spot price process. The parameters in their models are fitted to NordPool price data. Johnson and Barz [3] discuss 8 diffusion and jump diffusion models. By maximum likelihood methods these models are calibrated to the spot prices at four different energy markets.

The focus of all these models is to find appropriate stochastic processes to describe the spot price. An advantage of this approach is related to the abundance of price data, allowing the processes to be fitted directly to the observed prices series. It does not, however, take into account that the market in periods may be separated due to transmission constraints arising from the specific geographical distribution of supply and demand. Nor does it model the relation between the prices of the separated markets. Thus, the resulting price processes are not directly relevant for the individual market participants for which the nodal price differences are important.

Secondly, there are partial equilibrium models based on models of the underlying market and its transmission constraints, where market clearing nodal/area prices are found, given the geographical dispersion of supply and demand[2]. The main contribution is related to understanding the effect of nodal prices, as well as different methods for handling congestion. These models have however been inherently static, or two-periodic at most. Though congestion issues are well described, these models do not capture the underlying dynamics of the stochastic price processes, and can at most be regarded as giving a "snap shot" of the real world. In evaluating investments, production plans, etc. under uncertainty, these models do not provide a sufficient input to handle the challenges of future uncertainty.

In this paper, we seek to combine features of both these traditions, by introducing dynamics and stochastics into the static nodal price models, thus obtaining nodal price processes consistent with the physical rules of the transmission net. Demand and supply are represented by given price-elastic functions. Uncertainty is introduced by specifying demand or supply

[2] See for example, Bjørndal [2] and the references therein.

parameters as stochastic processes. A related idea is represented in Barlow [1], where the market price process is characterized on the basis of an inelastic demand market with a static functional form of the supply functions. We have in addition modelled an underlying three-node network, where the market is cleared by nodal prices. These nodal and system price processes may further be employed in analysing e.g. strategies of production or investments in net and production capacity when the nodal price is the relevant price.

The paper is organized as follows: Section 2 presents our model. Equilibrium prices are derived both in the presence and the absence of binding capacity constraints, and the system price and nodal prices are characterized. In section 3 we assume that the above market situation occurs repetitively with consecutive and independent market equilibria. We introduce uncertainty by characterizing demand as a stochastic function. Different choices of stochastic functions may represent different assumptions as to e.g. daily and seasonal variations. Based on the choice of stochastic process for demand in section 3, section 4 looks at the characteristics of the resulting stochastic nodal price processes, as well as discussing other applications of the model. Section 5 discusses different choices of model specification, while section 6 concludes the paper.

2 Price Formation in a Three-Node Electricity Market

Consider a simple three-node electricity market, with generation in node 1 and 2, and demand in node 3. The Generators in node 1 and 2 have the quadratic profit functions

$$\pi_i^s = p_i q_i^s - \frac{1}{2} c_i {q_i^s}^2. \tag{1}$$

Here p_i is the price, q_i^s is the quantity supplied, and c_i is the cost factor in node $i = 1, 2$. This gives the linear supply functions

$$p_i = c_i q_i^s \tag{2}$$

where production in each node, $q_i^s = \frac{1}{c_i} p_i$, follows directly from (2). All demand is consumed in node 3, i.e. $Q_D \equiv q_3^d$. Assuming no losses, in equilibrium aggregate supply $Q_S \equiv q_1^s + q_2^s$ equals aggregate demand, $Q_S = Q_D$. The implicit benefit of demand, π_3^d, for a given point of time is assumed to be of the form

$$\pi_3^d = (a - p_3) Q_D - \frac{1}{2} b {Q_D}^2, \tag{3}$$

giving the linear demand function

$$p_3 = a - b Q_D, \tag{4}$$

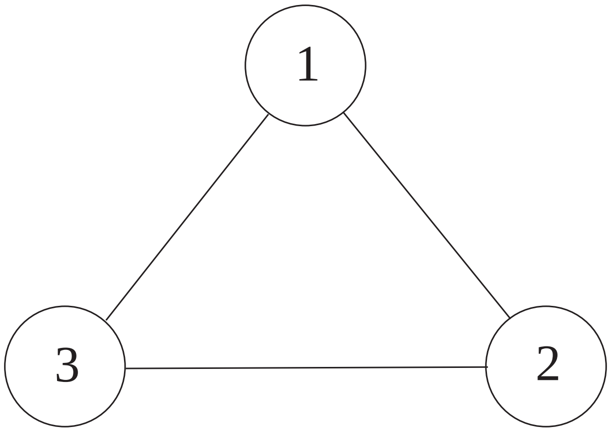

Figure 1: The network.

where $a, b > 0$. The consumed quantity in node 3 is therefore $Q_D = \frac{1}{b}(a - p_3)$ when the nodal price is p_3.

The three nodes are interconnected by a simple three-line "DC" network, as illustrated in figure 1. Each line is assumed to have identical technical characteristics and impedances equal to 1. The flows over each line are solely determined by physical laws. In our simple network the line flow over line ij in the direction from i to j resulting from production in node 1 and 2 are given by the equations[3]

$$\begin{aligned} q_{12} &= \frac{1}{3}q_1^s - \frac{1}{3}q_2^s \\ q_{13} &= \frac{2}{3}q_1^s + \frac{1}{3}q_2^s \\ q_{23} &= \frac{1}{3}q_1^s + \frac{2}{3}q_2^s. \end{aligned} \tag{5}$$

For flows in the opposite direction we have $q_{ji} = -q_{ij}$.

2.1 No capacity limits

Let us first assume that there are no capacity limits in the network. The challenge of the market is then to match supply and demand. In this case the market will be cleared at a common price $p_s = p_1 = p_2 = p_3$. This equilibrium price of a non-capacitated market is also termed the system

[3]These equations follow from three physical rules: Kirchhoff's Junction Rule, $q_i = \sum_{i \neq j} q_{ij}$ for $i = 1, 2$, states that the current flowing into any node is equal to the current flowing out of it. Following from Kirchhoff's Loop Rule we have $q_{13} = q_{12} + q_{23}$ which in the absence of losses states that the algebraic sum of flows over any path in a loop is equal. The Law of Conservation of Energy states that total generation equals total consumption, $q_3^d = q_1^s + q_2^s$.

price. The aggregate supply curve as a function of the market price p_s is

$$Q_S = \frac{1}{c} p_s \tag{6}$$

where $c \equiv \frac{c_1 c_2}{c_1 + c_2}$ is the resulting cost factor of aggregate supply. The proportion of total generation generated in node i is now $\alpha_i \equiv \frac{q_i^s}{q_1^s + q_2^s}$. By inserting (2) we have the production weights

$$\alpha_i = \frac{c_{(3-i)}}{c_1 + c_2} \qquad \text{for } i = 1, 2. \tag{7}$$

The market is cleared at the price which matches supply and demand, i.e. for $Q_S = Q_D$, where Q_D is given by (4) and Q_S by (6). The equilibrium price, the system price, is thus given by $p_s = \frac{ac}{b+c}$, giving

$$p_s = \frac{a c_1 c_2}{b c_1 + b c_2 + c_1 c_2}. \tag{8}$$

The corresponding total equilibrium quantity is given by $Q_S = Q_D = \frac{a}{b+c}$, i.e.

$$Q_S = Q_D = \frac{a(c_1 + c_2)}{b c_1 + b c_2 + c_1 c_2}. \tag{9}$$

In this unrestrained solution the proportions of the total production produced in node 1 and 2 are given by the least-cost production mix α_1 and α_2 of (7). Thus, nodal production is $q_i^s = \frac{\alpha_i a}{b+c}$, giving

$$q_i^s = \frac{a c_{3-i}}{b c_1 + b c_2 + c_1 c_2} \qquad \text{for } i = 1, 2 \tag{10}$$

By inserting the above flow quantities into the line flow equations (5), we find the line flows in an unrestricted market clearing:

$$\begin{aligned} q_{12} &= \frac{a(c_2 - c_1)}{3(b c_1 + b c_2 + c_1 c_2)} \\ q_{13} &= \frac{a(c_1 + 2c_2)}{3(b c_1 + b c_2 + c_1 c_2)} \\ q_{23} &= \frac{a(2c_1 + c_2)}{3(b c_1 + b c_2 + c_1 c_2)}. \end{aligned} \tag{11}$$

2.2 Capacity limit on line 12

In the case of capacity limits in the network, the optimal market equilibrium is defined as the allocation that maximizes social surplus, given the constraints of the network. Now let us assume that the capacity of line 12 is restricted to $\widehat{C}$ for flows in either direction, while the capacity of the other lines will not be binding. The capacity of line 12 will thus be binding for any combination of parameters that satisfy the inequality $|q_{12}| > \widehat{C}$, i.e.

$$\left| \frac{a(c_2 - c_1)}{3(bc_1 + bc_2 + c_1 c_2)} \right| > \widehat{C}. \tag{12}$$

In section 3 we will assume a repetitive market where the intersect a of the demand curve is stochastic. The slope of demand and supply curves, b, c_1, and c_2, are for simplicity chosen to be constants. In this setting it is therefore the level of a that determines whether the capacity limit of line 12 will be binding. To simplify, let us define the producer in node 1 as the least cost producer assuming that $c_1 < c_2$. This implies that $q_1^s > q_2^s$ with a constant direction of the line flow on line 12, i.e. $q_{12} \geq 0$. Clearing the market at a uniform price the constraint on line 12 becomes binding when the demand reaches the level which solves $q_{12}(\hat{a}) = \widehat{C}$. This critical demand intersect level is

$$\hat{a} = 3\widehat{C}\frac{bc_1 + bc_2 + c_1 c_2}{c_2 - c_1}. \tag{13}$$

By inserting $\hat{a}$ from (13) into (9) and (10) we find the corresponding levels of production in node 1 and 2, $\hat{q}_1^S$ and $\hat{q}_2^S$, and consumption, $\hat{Q}_D$;

$$\hat{q}_i^S = 3\widehat{C}\frac{c_{3-i}}{c_2 - c_1} \qquad \text{for } i = 1, 2 \tag{14}$$

$$\hat{Q}_D = 3\widehat{C}\frac{c_1 + c_2}{c_2 - c_1}. \tag{15}$$

For a realization of $a \leq \hat{a}$ the unrestrained solution resulting from a common market price p_s is feasible. At $a = \hat{a}$ the line q_{12} is fully utilized, and the unrestrained market solution with the above quantities of (14) and (15) is feasible. This quantity, $\hat{Q}_D = \hat{Q}_S$ is the maximum feasible aggregate production given the production mix α_1 and α_2 of the unrestrained solution, which also is the minimum-cost production mix.

A demand realization $a > \hat{a}$ calls for a higher total production and consumption. The unrestrained solution based on a uniform market price p_s is however now not feasible. Still, it is in fact possible to achieve higher production levels, i.e. $Q_S > \hat{Q}_S$ without violating the capacity constraints of line 12. The clue is to define differentiated nodal prices and change the production mix. This can be seen by studying the line flows resulting from Kirchhoff's law. For each extra unit produced in node 1, equation (5) states that $\frac{1}{3}$ of the quantity will flow on line 12 from node 1 to node 2. This action alone is not possible if the line is already congested. We however find that equation (5) also states that for each extra unit produced in node 2, $\frac{1}{3}$ of this quantity will flow on line 12 from node 2 to node 1. Additional quantities $(Q_S - \hat{Q}_S)$ are thus feasible by producing equal additional amounts in each node, i.e. with the production mix $\hat{\alpha}_1 = \hat{\alpha}_2 = \frac{1}{2}$.

We have a new kinked aggregate supply curve, which for quantities above $\hat{Q}_S$ reflects the marginal cost of additional production using the new production mix. For any aggregate production $Q_S > \hat{Q}_S$ (occurring when $a > \hat{a}$), the production in node i is given by $q_i^s = \alpha_i \hat{Q}_S + \hat{\alpha}_i (Q_S - \hat{Q}_S)$, i.e. with the least cost mix α_i for the critical level of non-congested quantity, and a mix of $\hat{a}_i = \frac{1}{2}$ for any additional quantity. By substituting for $\hat{Q}_S$, α_i, and $\hat{\alpha}_i$, the feasible nodal production as a function of any total production $Q_S > \hat{Q}_S$ is

$$q_i = \frac{1}{2} Q_S + (3 - 2i) \frac{3}{2} \widehat{C} \qquad \text{for } i = 1, 2. \tag{16}$$

For $Q_S > \hat{Q}_S$, the aggregate cost of production, $\Pi_C = \frac{1}{2} \sum_{i=1,2} c_i {q_i^s}^2$ is

$$\Pi_C = \frac{1}{2} \sum_{i=1,2} c_i \left[\alpha_i \hat{Q}_S + \hat{\alpha}_i (Q_S - \hat{Q}_S) \right]^2 \tag{17}$$

giving the marginal cost of

$$\frac{\partial \Pi_C}{\partial Q_S} = \frac{1}{4}(c_1 + c_2) Q_S + \frac{3}{4}(c_1 - c_2) \widehat{C}_{12}. \tag{18}$$

The aggregate benefit of consumption, Π_B, is given by omitting the payments in (3), i.e. $\Pi_B = a Q_D - \frac{1}{2} b {Q_D}^2$, giving the marginal benefit of consumption

$$\frac{\partial \Pi_B}{\partial Q_D} = a - b Q_D.$$

By equating the marginal cost of aggregate production and the marginal benefit of consumption, we find the equilibrium amount $Q^* = Q_S = Q_D$ for $a > \hat{a}$ to be

$$Q^* = \frac{4a - 3\widehat{C}(c_1 - c_2)}{4b + c_1 + c_2}. \tag{19}$$

Given the equilibrium amount Q^* the quantities in each node are found by (4) and (16).

To achieve these quantities and balance the resulting regional markets, it is necessary to operate with nodal prices tailored to induce the required quantities. Prices in node 1 and 2 are given by the individual supply curves of (2), $p_i = c_i q_i^s$. For $a > \hat{a}$ prices as a function of the total quantity supplied are

$$p_1 = c_1 \left(\frac{1}{2} Q_S + \frac{3}{2} \widehat{C}\right) \tag{20}$$

$$p_2 = c_2 \left(\frac{1}{2} Q_S - \frac{3}{2} \widehat{C}\right). \tag{21}$$

The nodal price in node 3 is given by (4).

2.3 Nodal prices as a function of the demand parameter a

To sum up, the market price is dependent on the realization of the demand parameter a. The market price in a non-capacitated market, i.e. when $a \leq \hat{a}$, is given by (8); $p_s = \frac{ac_1c_2}{b(c_1+c_2)+c_1c_2}$. By inserting Q^* into (4), (20) and (21), we obtain the nodal prices of the capacitated market when $a > \hat{a}$. The nodal prices as a function of the demand parameter a can be summarized by

$$p_1 = \begin{cases} p_s & \text{for} \quad a \leq \hat{a} \\ \frac{c_1(2a+3\widehat{C}(2b+c_2))}{4b+c_1+c_2} & \text{for} \quad a > \hat{a} \end{cases} \tag{22}$$

$$p_2 = \begin{cases} p_s & \text{for} \quad a \leq \hat{a} \\ \frac{c_2(2a-3\widehat{C}(2b+c_1))}{4b+c_1+c_2} & \text{for} \quad a > \hat{a} \end{cases} \tag{23}$$

$$p_3 = \begin{cases} p_s & \text{for} \quad a \leq \hat{a} \\ \frac{a(c_1+c_2)+3\widehat{C}b(c_1-c_2)}{4b+c_1+c_2} & \text{for} \quad a > \hat{a} \end{cases} \tag{24}$$

where $\hat{a}$ is given by equation (13). The corresponding production and consumption in the three nodes are given by inserting prices into the individual supply and demand functions, i.e. $q_1^s = \frac{1}{c_1}p_1(a)$, $q_2^s = \frac{1}{c_2}p_2(a)$, and $Q_D = \frac{1}{b}(a - p_3(a))$.

In figure 2 the prices are plotted for different levels of a for a model where $b = 0.05$, $c_1 = 0.2$, $c_2 = 0.8$, and $\widehat{C} = 120$, implying that $\hat{a} = 126$. Due to the simple model setup the functions are all piecewise linear in a. When the line capacity is not fully utilized, the market is cleared at the common market price, p_s. For higher demand levels, $a > \hat{a}$, prices in node 1 are set lower than the system price to curb production and reduce the flow in the direction from 1 to 2, while prices in node 2 are set higher than p_s to relieve capacity problems by inducing a greater counterflow on line 12.

3 Introducing dynamics and uncertainty

Our aim is now to analyse the effect of limited grid capacity on nodal price processes. Prices at a given point of time are given by (22)-(24) above[4]. Basically, uncertainty in prices is driven by the uncertainty of underlying fundamentals related to demand and/or supply. To focus on the basic effect of grid constraints, we have introduced uncertainty in the demand function (4) only, keeping a transparent and controllable model. Uncertainty is implemented by defining a as a stochastic function. From the definition of the demand function it is clear that shifts in a represent parallel shifts in the

[4]Note that the allocation of production and consumption at each instant is as in the static model described above, implying that none of the market participants in this model act strategically over time.

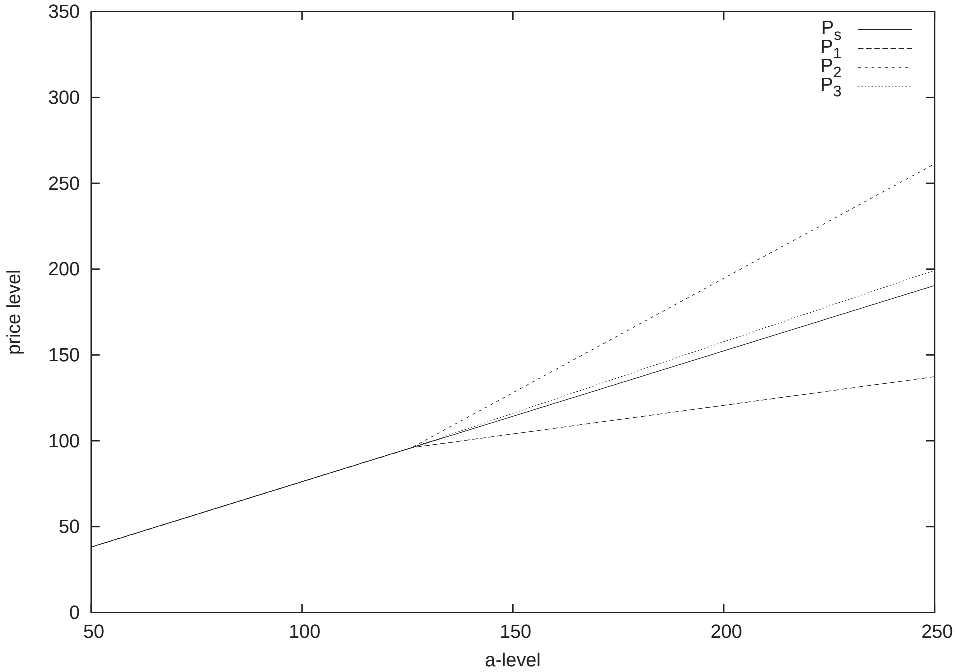

Figure 2: Plot of prices as a function of the a-parameter.

demand function. In a market with electrical household heating, the most natural example could be the temperature. By defining a stochastic process for a, and assuming that the process a takes only admissible values (e.g. $a > 0$), equations (22)-(24) will define the stochastic processes for p_1, p_2, and p_3.

In order to derive the nodal price processes, we must first define a stochastic process for our fundamentals, in this case the parameter a_t. Finding a good representation of the real-world stochastic process is not a simple task. It is important to have a clear understanding of the effects we want the model to capture, and also how a reasonable process should evolve. Several questions arise in this context, for example; - Is the real world process explicitly time dependent? - What is the level of the process expected to be at a given point of time? - How volatile is the process? - Is the noise constant, or is it dependent on time and/or the level of the process? - Does the driving process display periodic patterns? - Is the driving process mean reverting, and if so, how fast on average?

In our paper we do not, however, aim for ultimate realism in any particular market. For computational tractability we employ a continuous time framework. We have chosen to model the parameter a_t by a particular continuous time Itô diffusion, namely a time dependent mean reverting

(Ornstein-Uhlenbeck) process of the form

$$da_t = \gamma_t(\eta_t + \frac{\eta_t'}{\gamma_t} - a_t)dt + \sigma_t dW_t. \tag{25}$$

Here W_t is a Brownian motion, γ_t is related to the speed of mean reversion and η_t is the "on average" seasonal process level. Variants of this process are used extensively in the literature, see e.g. Lucia and Schwartz [4] or Johnson and Barz [3], while the above formulation is based on Lund and Ollmar [5]. This process captures several important properties of a demand curve for electricity. The process is mean reverting, giving demand a tendency to normalize after some time, an attribute which is characteristic of demand. By choosing a rather high γ_t, the process would relatively rapidly be driven towards the average seasonal process level, a lower γ_t causes a slow drive towards the average level. As we will see below, this process formulation also opens for specifying cyclical patterns of demand. Note that the Ornstein-Uhlenbeck formulation above implies that volatility represented by $\sigma_t dW_t$ is independent of a_t. Though this process captures many important aspects of demand, it may attain negative values, requiring caution as to applications where this may be problematic.

For $s < t$ the explicit solution of equation (25) is

$$a_t = (a_s - \eta_s)e^{-\int_s^t \gamma_u du} + \eta_t + \int_s^t \sigma_u e^{-\int_u^t \gamma_r dr} dW_u \tag{26}$$

We now simplify by letting $\gamma_t \equiv \gamma$ and $\sigma_t \equiv \sigma$, that is, constant volatility and a constant speed of mean reversion. Since σ is deterministic, the Itô integral is normally distributed and we can write a_t as

$$a_t = (a_s - \eta_s)e^{-\gamma(t-s)} + \eta_t + \sigma(\frac{1 - e^{-2\gamma(t-s)}}{2\gamma})^{1/2}\varepsilon \tag{27}$$

where ε is a standard normal distributed random variable. For a given a_s, the Gaussian process a_t has an conditional mean and variance[5] at time $t > s$ equal to

$$\mu_t = (a_s - \eta_s)e^{-\gamma(t-s)} + \eta_t \tag{28}$$

$$\rho_t = \sigma^2 \cdot (\frac{1 - e^{-2\gamma(t-s)}}{2\gamma}). \tag{29}$$

Since the expected value of a_t is equal to η_t when $t \to \infty$, we can interpret this as the long run mean level for the process.

Demand clearly follows several cyclical patterns over time, reflecting patterns of nature as well as human activity that vary over the day, the week

[5] To simplify notation we suppress the s, a_s dependence in μ, ρ. Still they must always be seen as functions of these variables.

and across the year. In our model, price variations are induced by these variations in demand. These fluctuations may be modelled by including several trigonometric functions with different parameters. We have specified the average seasonal process level, η_t, as

$$\eta_t = A_0 + \sum_{j=1}^{k} \{A_j \cos(\omega_j t) + B_j \sin(\omega_j t)\}.$$

where the parameters of A_j, B_j and the frequencies ω_j are chosen to specify the k different patterns we wish to model.

In the paper Lund and Ollmar [5] the process is calibrated to the spot price at the Nordic electricity marked. Here one unit of time corresponds to one hour, and the frequencies are set to

$$\begin{array}{lllllll} \omega_1 & = & 2\pi/8760 & \omega_2 & = & 2\omega_1 & \text{(year)} \\ \omega_3 & = & 2\pi/168 & \omega_4 & = & 2\omega_3 & \text{(week)} \\ \omega_5 & = & 2\pi/24 & \omega_6 & = & 2\omega_5 & \text{(day)} \end{array}$$

to model yearly, weekly and daily variations in the spot price. Demand variation highly matches that of the spot prices. To illustrate how our model may be applied, we therefore use approximately the same parameters as Lund and Ollmar, this time to model the demand process a[6].

The two lower panels of figure 3 show the resulting (time varying) long term mean level of the demand parameter a_t. In the first of these panels, covering five weeks, we are able to see the resulting daily and weekly variations in the mean, while in the second covering fifty weeks, we are able to see yearly variations in a_t. In the two upper panels of figure 3 we have plotted a realization of the process for $a_0 = 80.0$, $\sigma = 2.0$.

4 The stochastics of nodal prices - Characteristics and applications

The price process of our model is driven by the variations in the demand parameter a. The nodal price processes are thus completely defined by the price equations (22)-(24) together with the stochastic process of a_t given by equation (27). Based on this characterization of the nodal price processes, we have a tool useful for several purposes. Within a given model, we are able to study the stochastic properties of nodal prices, as well as performing numerical and analytical analyses of different issues in the market. The

[6]The parameters chosen for A and B are calibrated to reflect the level estimated in [5]: $A_1 = 32.2$, $A_2 = -8.4$, $A_3 = -3.1$, $A_4 = -0.2$, $A_5 = -5.3$, $A_6 = 1.6$, $B_1 = -3.7$, $B_2 = 12.3$, $B_3 = 4.1$, $B_4 = 2.8$, $B_5 = -4.8$, and $B_6 = -4.2$. Apart from this, the remaining parameters are chosen to fit our example, with the reversion parameter γ set to 0.01 and $A_0 = 100.0$.

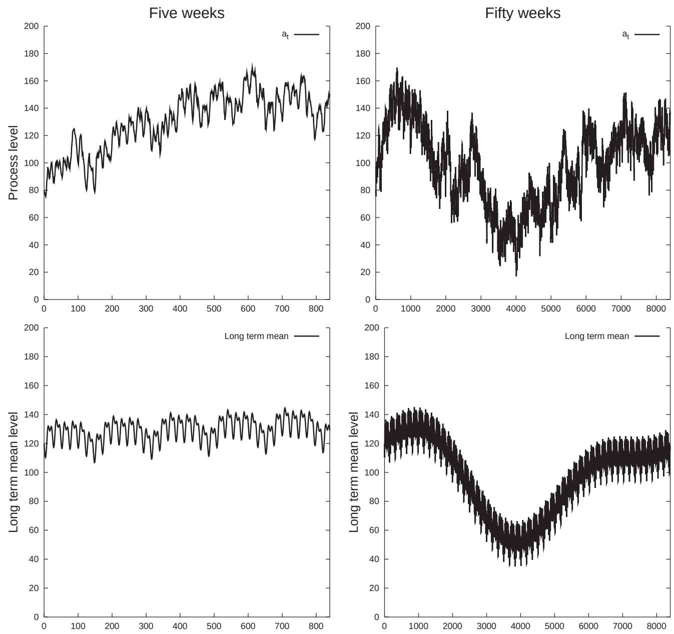

Figure 3: Plot of one replicate of the a-process, together with its long term mean level.

purpose of this paper has been to gain insight into how grid limitations influence the underlying stochastic nodal price processes. In this section we will briefly sketch some applications.

- In figure 4 we have illustrated the realization of the price process for the above realization of a_t. This is but one possible replicate of the price processes. More interestingly, our characterization of the price processes allows us to calculate e.g. expected levels of nodal prices, as well as the estimated volatility of prices. This is information which is important input in evaluating power contracts, investment decisions or other applications for which future prices are important.

  As an illustration, assume that we want to find the expected price levels in this model, given the current level of demand a_s. With the notation introduced in the appendix we can write price expectations

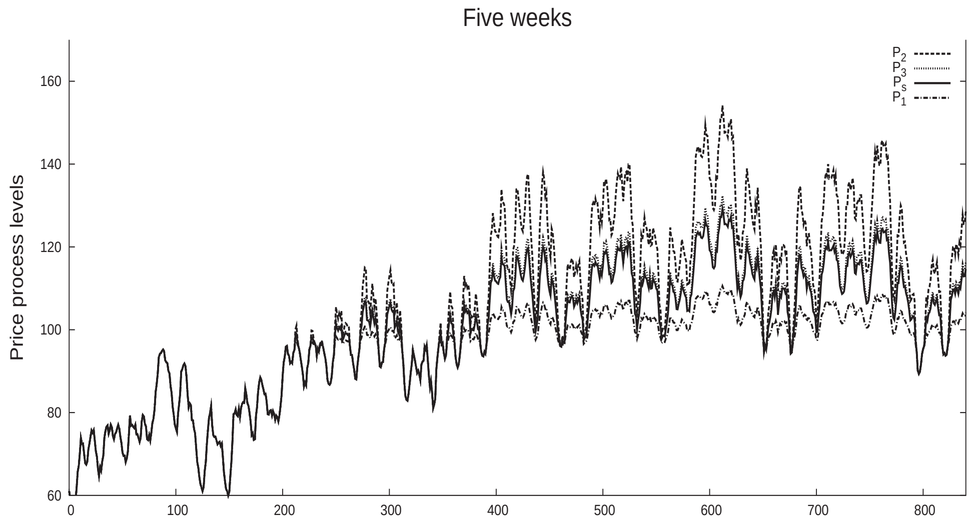

Figure 4: Price evolution for this a-replicate.

as

$$
\begin{aligned}
E[P_S(t)|a_s] &= \frac{c_1c_2}{\Psi}\mu_t \\
E[P_1(t)|a_s] &= E[P_S(t)I_{\{a_t\le\hat{a}\}}|a_s] + \frac{2c_1}{\Phi}E[a_tI_{\{a_t>\hat{a}\}}|a_s] \\
&\quad +3\frac{c_1}{\Phi}\widehat{C}(2b+c_2)E[I_{\{a_t>\hat{a}\}}|a_s] \\
&= \frac{c_1c_2}{\Psi}\bar{A}_t + \frac{2c_1}{\Phi}(\mu_t-\bar{A}_t) + 3\frac{c_1}{\Phi}\widehat{C}(2b+c_2)(1-\mathcal{G}(\frac{\hat{a}-\mu_t}{\sqrt{\rho_t}})) \\
E[P_2(t)|a_s] &= \frac{c_1c_2}{\Psi}\bar{A}_t + \frac{2c_2}{\Phi}(\mu_t-\bar{A}_t) - 3\frac{c_2}{\Phi}\widehat{C}(2b+c_1)(1-\mathcal{G}(\frac{\hat{a}-\mu_t}{\sqrt{\rho_t}})) \\
E[P_3(t)|a_s] &= \frac{c_1c_2}{\Psi}\bar{A}_t + \frac{c_1+c_2}{\Phi}(\mu_t-\bar{A}_t) + 3\frac{\widehat{C}b(c_1-c_2)}{\Phi}(1-\mathcal{G}(\frac{\hat{a}-\mu_t}{\sqrt{\rho_t}})),
\end{aligned}
$$

where $\Phi = b(c_1+c_2)+c_1c_2$, $\Psi = 4b+c_1+c_2$ and $\mathcal{G}$ denotes the cumulative standard normal distribution function. The price expectation functions are plotted in figure 5.

Likewise, the volatility of the price processes may be calculated in a similar manner. For example, again with notation from appendix A,

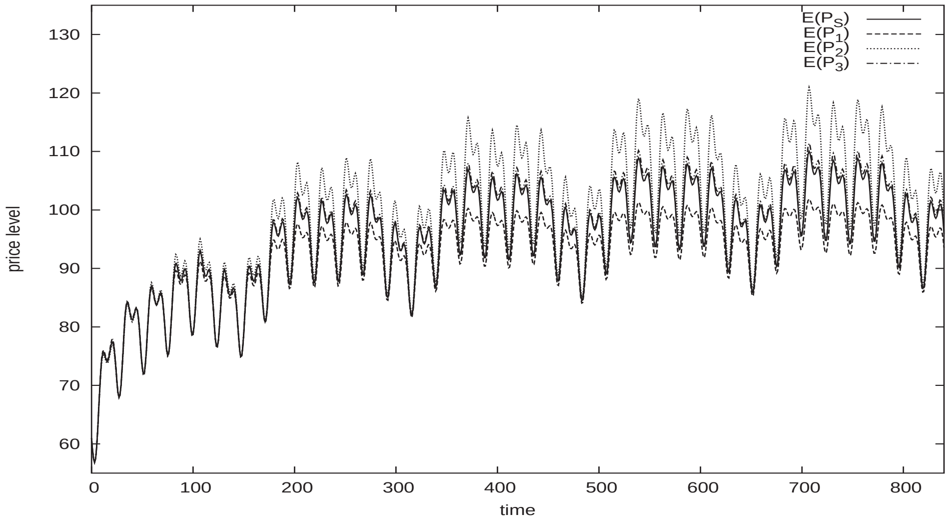

Figure 5: The expected nodal prices.

we have that

$$\begin{aligned}
\mathbf{Var}\left[P_S(t)\right] &= \frac{(c_1c_2)^2}{\Psi^2}\mathbf{Var}\left[a(t)\right] = \frac{(c_1c_2)^2}{\Psi^2}\rho_t \\
\mathbf{Var}\left[P_1(t)\right] &= E\left[(P_S(t) - E[P_S(t)])^2 I_{\{a_t \le \hat{a}\}}\right] \\
&\quad + \frac{(2c_1)^2}{\Phi^2}E\left[(a_t - E[a_t])^2 I_{\{a_t > \hat{a}\}}\right] \\
&= \frac{(c_1c_2)^2}{\Psi^2}(\bar{C}_t - 2\bar{A}_t\mu_t + \bar{F}_t\mu_t^2) \\
&\quad + 4\frac{c_1^2}{\Phi^2}(\bar{D}_t - 2\bar{B}_t\mu_t + (1-\bar{F}_t)\mu_t^2),
\end{aligned}$$

given the state a_s at time s.

- Price differences are highly important for producers operating in several regions, as well as producers and consumers hedging their positions for example by derivative contracts written on the system price. Figure 6 shows the price differences between the nodal prices and the non-constrained system price. In this realization, we find an initial period where the demand has not led to binding network constraints, while the following time periods show differentiated nodal prices. Our model allows the price difference processes to be explicitly analysed, for example by calculating expectation and variance functions, and applying these in evaluating contracts and market positions.

- Another useful application is to estimate the degree to which the grid will be congested in a given time period. Let $F_{\hat{a}}([\hat{S}, T])$ be the expected

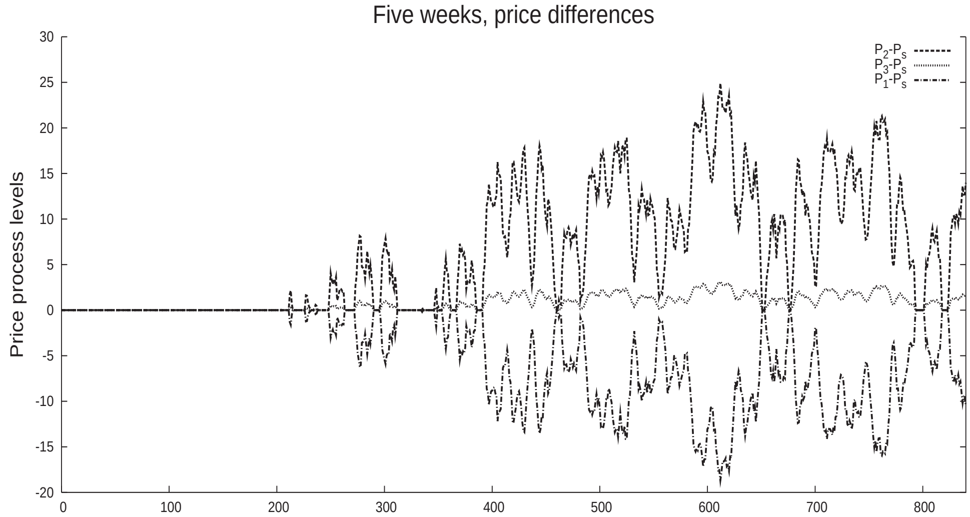

Figure 6: Evolution of price differences.

fraction of hours with nodal prices in the future period $[\hat{S}, T]$, $\hat{S} > s$. Within our setup this can be calculated as follows:

$$\begin{aligned} F_{\hat{a}}([\hat{S}, T]) &= \frac{1}{T-\hat{S}} E[\int_{\hat{S}}^{T} I_{\{a_t > \hat{a}\}} dt | a_s] \\ &\overset{\text{Fubini}}{=} \frac{1}{T-\hat{S}} \int_{\hat{S}}^{T} E I_{\{a_t > \hat{a}\}} | a_s] dt \\ &= \frac{1}{T-\hat{S}} \int_{\hat{S}}^{T} (1 - \mathcal{G}(\frac{\hat{a}-\mu_t}{\sqrt{\rho_t}})) dt \\ &= 1 - \frac{1}{T-\hat{S}} \left\{ \left[t\mathcal{G}(\frac{\hat{a}-\mu_t}{\sqrt{\rho_t}}) \right]_{\hat{S}}^{T} \right. \\ &\quad \left. - \int_{\hat{S}}^{T} t\, (\frac{\hat{a}-\mu_t}{\sqrt{\rho_t}})' \, \frac{1}{\sqrt{2\pi\rho_t}} e^{-\frac{(\hat{a}-\mu_t)^2}{2\rho_t}} dt \right\} \end{aligned}$$

where μ_t, ρ_t are seen as functions of the initial process level a_s as in (28) and (29). With the parameter values from the previous example, we find that

$$F_{126}([0, 336]) = 0.29$$

by numerical integration. That is, we would expect nodal prices in 29% of the hours the first two weeks when $\widehat{C} = 120$ (or alternatively, $\hat{a} = 126$).

- Other applications of the model involve analysing the sensitivity of changes in model parameters on price expectations, volatility etc. This

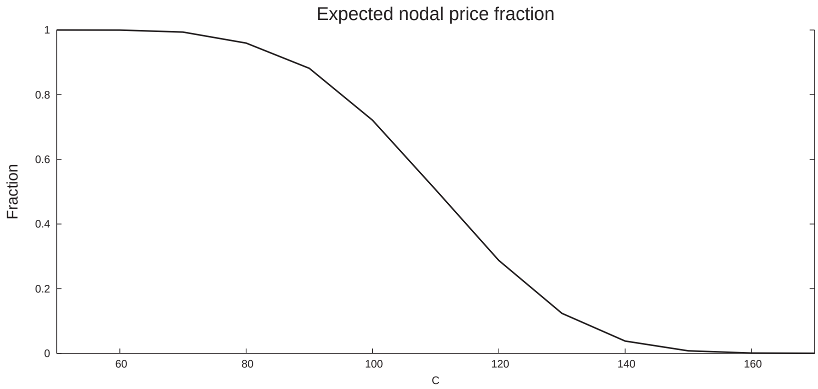

Figure 7: Expected fraction of the hours with nodal prices in the two first weeks, as a function of the capacity.

may be done by analytic or numerical studies of the consequences of changing the model parameters, as for example related to the demand slope or cost parameters, or changing the capacity of the grid. For example, in figure 7 we show how the expected fraction of nodal prices varies by varying the capacity $\widehat{C}$ of the congested line[7].

5 Other model specifications

Above we have illustrated some of the main issues in modelling stochastic nodal prices. The model may be extended in several directions, for example with respect to the network, the representation of supply and demand, as well as the choice and modelling of stochastic parameters. In applying the principles of the model to analyse more complex real world problems, the challenge is to simplify, but yet capture the key features of the problem. It is then important to have a clear idea of which effects we want to analyse. Also, note that several extensions of the model will necessitate numerical simulation rather than analytical characteristics of the nodal price processes. Below we will shortly discuss possible model extensions.

Network: The 3-node network is simple. Still it may for example be seen as an approximation to the Norwegian/Swedish part of the Nordic market, where zonal aggregation often has been applied with two Norwegian zones, and one Swedish zone. By applying slightly more complex networks, we may similarly be able to pinpoint key features of the networks in other countries.

[7]See Lund and Rud [6] for an analysis within this framework related to investments in grid capacity.

Demand and Supply Functions: By modelling demand and supply in the same node, problems of negative quantities will be avoided, as a negative net demand simply indicates net production. Further, other demand and supply functions may be implemented, though linear demand and supply functions facilitate a clear and simple model.

Stochastic processes: For the demand process a_t above, we have chosen a simple process. Clearly more complex process could be applied. a_t could also be a process defined by combinations of other (possibly correlated) processes. As an illustration suppose that demand consists of household and industrial consumption. Let us assume that the industrial consumption varies slowly due to changing market conditions, and this is modelled by a reverting process X. Household consumption, on the other hand, is exposed to temperature variations, and this could be modelled by a more volatile stochastic process Y, normalizing relatively quickly. It may then be appropriate to use a process e.g. of the form $a_t = \beta_1 X_t + \beta_2 Y_t$. Clearly these processes could also incorporate long-term trends.

In another model we could be particularly interested in the effects of demand variations throughout the day. We know that day and night variation in demand may be large in some periods and smaller in others. It is also often the case that the consumption during the night has low variance, while the peak consumption varies much more. This could be captured by introducing stochastic amplitudes in demand. As a simple illustration consider $Y_t = 50 + X_t(1.2 + \sin(2\pi \frac{t}{24}))$, where $X_t > 0$ is a process reverting at 50. This leads to periods with high prices at day time, with low fluctuations in the night as seen in figure 8.

In section 2.3 we focused on the nodal prices as functions of the parameter a. Clearly we could have considered the prices as functions of the other parameters, as for example the demand slope, or production parameters.

6 Conclusions

In this paper we have demonstrated how capacity limits in the grid influence the stochastic price processes. Based on an intuitive model for the demand dynamics, we have shown how our framework can help analyse the characteristics of the price processes. We have also indicated possible applications of the model.

This paper can be seen as a "primer" for introduction of dynamics and uncertainty in a nodal network. In the paper we focused on examples to illustrate how the model could be applied. The main focus has been on simplicity, rather than realism. Still we have given indications of possible generalisations that could be important when real world problems are studied.

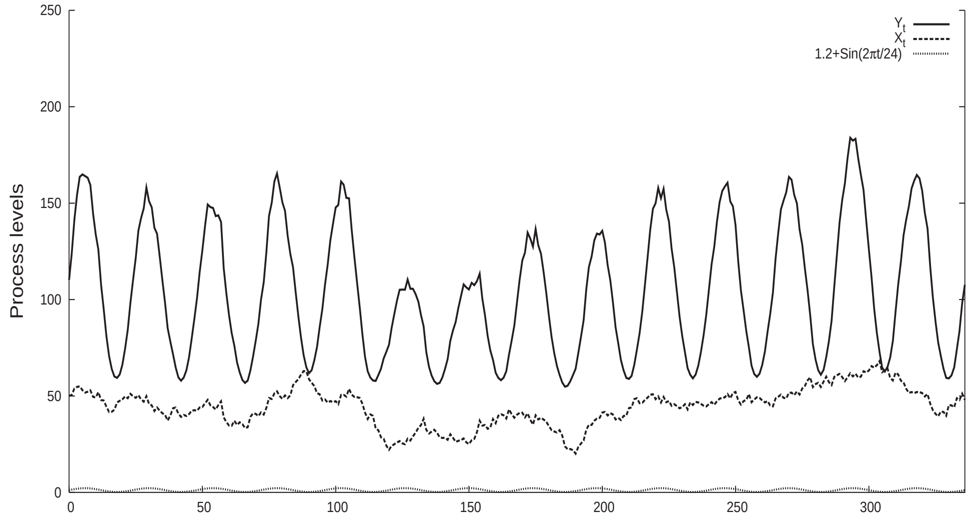

Figure 8: Plot of a process with large volatility in daytime.

As the fundamental processes can be unobservable in practise, it may be difficult to calibrate our model to fit observed nodal prices. Compared to models based on observed nodal prices, our approach may be advantageous in several cases. As an illustration we point out that our model may give insight in problems where there are no observations, for instance for other potential grid specifications. It is also simple to include subjective beliefs about the future market situation. Clearly this is highly relevant for investment decisions. In addition note that a naïve calibration of the price process directly from data may give strange results, for instance price movements in neighbouring nodes that are physically impossible. In our model, the dynamics will always be consistent with the underlying physical grid.

Appendix

In this section we compute some useful expectations. An important function is $I_{\{a_t \leq \hat{a}\}}$ which is 1 when $a_t \leq \hat{a}$, i.e. when there is no congestion and non-differentiated nodal prices, and 0 otherwise indicating a congested net. Assume $t > s$, and that we know a_s. When a is modelled by the Ornstein-Uhlenbeck process, we know that it is Gaussian with mean and variance given by equations (28) and (29). Therefore the probability that the net is un-congested at time t, given present state a_s, can be written as

$$\begin{aligned}
\bar{F}_t \equiv E[I_{\{a_t \leq \hat{a}\}}|a_s] &= \int_{-\infty}^{\hat{a}} \frac{1}{\sqrt{2\pi\rho_t}} e^{-\frac{(x-\mu_t)^2}{2\rho_t}} dx \\
&= \mathcal{G}^{\mu_t,\rho_t}(\hat{a}) \\
&= \mathcal{G}(\frac{\hat{a}-\mu_t}{\sqrt{\rho_t}}),
\end{aligned}$$

where $\mathcal{G}$ denotes the cumulative standard normal distribution function.

For calculating price expectations etc., we need several calculations. Recall that $\hat{a}$ is defined by (13), and that ρ_t and μ_t depend on s and a_s. We further calculate $E[a_t|a_s, a_t \leq \hat{a}] \equiv E[a_t \cdot I_{\{a_t \leq \hat{a}\}}|a_s]$:

$$\begin{aligned}
\bar{A}_t \equiv E[a_t \cdot I_{\{a_t \leq \hat{a}\}}|a_s] &= \frac{1}{\sqrt{2\pi\rho_t}} \int_{-\infty}^{\hat{a}} x e^{-\frac{(x-\mu_t)^2}{2\rho_t}} dx \\
&= \frac{1}{\sqrt{2\pi\rho_t}} \int_{-\infty}^{\hat{a}} (x-\mu_t) e^{-\frac{(x-\mu_t)^2}{2\rho_t}} dx \\
&\quad +\mu_t \int_{-\infty}^{\hat{a}} \frac{1}{\sqrt{2\pi\rho_t}} e^{-\frac{(x-\mu_t)^2}{2\rho_t}} dx \\
&= -\frac{\sqrt{\rho_t}}{\sqrt{2\pi}} e^{-\frac{(\hat{a}-\mu_t)^2}{2\rho_t}} + \mu_t \mathcal{G}(\frac{\hat{a}-\mu_t}{\sqrt{\rho_t}}).
\end{aligned}$$

Clearly $\bar{B}_t \equiv E[a_t \cdot I_{\{a_t > \hat{a}\}}|a_s] = E[a_t|a_s] - \bar{A}_t = \mu_t - \bar{A}_t$.

In addition

$$E[a_t^2|a_s] = \rho_t + \mu_t^2,$$

and

$$\begin{aligned}
\bar{C}_t \equiv E[a_t^2 \cdot I_{\{a_t \leq \hat{a}\}}|a_s] &= \frac{1}{\sqrt{2\pi\rho_t}} \int_{-\infty}^{\hat{a}} (x-\mu_t)^2 e^{-\frac{(x-\mu_t)^2}{2\rho_t}} dx \\
&\quad +2\frac{\mu_t}{\sqrt{2\pi\rho_t}} \int_{-\infty}^{\hat{a}} (x-\mu_t) e^{-\frac{(x-\mu_t)^2}{2\rho_t}} dx \\
&\quad +\mu_t^2 \int_{-\infty}^{\hat{a}} \frac{1}{\sqrt{2\pi\rho_t}} e^{-\frac{(x-\mu_t)^2}{2\rho_t}} dx \\
&= -\frac{\sqrt{\rho_t}}{\sqrt{2\pi}} (\hat{a}-\mu_t) e^{-\frac{(\hat{a}-\mu_t)^2}{2\rho_t}} + \rho_t \mathcal{G}(\frac{\hat{a}-\mu_t}{\sqrt{\rho_t}}) \\
&\quad -\frac{2\mu_t\sqrt{\rho_t}}{\sqrt{2\pi}} e^{-\frac{(\hat{a}-\mu_t)^2}{2\rho_t}} + \mu_t^2 \mathcal{G}(\frac{\hat{a}-\mu_t}{\sqrt{\rho_t}}) \\
&= -\frac{\sqrt{\rho_t}}{\sqrt{2\pi}} (\hat{a}+\mu_t) e^{-\frac{(\hat{a}-\mu_t)^2}{2\rho_t}} + (\mu_t^2+\rho_t) \mathcal{G}(\frac{\hat{a}-\mu_t}{\sqrt{\rho_t}}).
\end{aligned}$$

Also observe that

$$\bar{D}_t \equiv E[a_t^2 \cdot I_{\{a_t > \hat{a}\}}|a_s] = E[a_t^2|a_s] - E[a_t^2 \cdot I_{\{a_t \leq \hat{a}\}}|a_s].$$

References

[1] Martin T. Barlow. A diffusion model for electricity prices. *Mathematical Finance*, 12(4):287–298, October 2002.

[2] Mette Bjørndal. *Topics on Electricity Transmission Pricing*. PhD thesis, Norwegian School of Economics and Business Administration, 2000.

[3] Blake Johnson and Graydon Barz. Selecting stochastic processes for modelling electricity prices. In *Energy Modelling And The Management Of Uncertainty*, pages 3–21. RISK Books, 1999.

[4] Julio J. Lucia and Eduardo S. Schwartz. Electricity prices and power derivatives: Evidence from the nordic power exchange. *Review of Derivatives Research*, 5(1):5–50, 2002.

[5] Arne-Christian Lund and Fridthjof Ollmar. Analysing flexible load contracts in the energy market. Discussion paper, http://www.nhh.no/for/dp/ 2002/1802.pdf, 2002.

[6] Arne-Christian Lund and Linda Rud. Understanding the stochastics of nodal prices: Investments and price processes in a constrained network. Unpublished working paper, 2004.

[7] F. C. Schweppe, M. C. Caramanis, R. D. Tors, and R. E. Bohn. *Spot Pricing of Electricity*. Kluwer Academic Publishers, 1988.

[8] R. Weron, M. Bierbrauer, and S. Trück. Modeling electricity prices: jump diffusion and regime switching. *Physica A*, (336):39–48, 2004.